

Title No. 113-S40

# Reliability of Temperature-Dependent Models for Analysis of Reinforced Concrete Members Subjected to Fire

by Fady EIMohandes and Frank J. Vecchio

*A computational modeling procedure has been developed for better estimating the behavior of reinforced concrete members subjected to fire. The highly nonlinear procedure of combined thermal and structural analysis integrates the transient conductive, boundary-convective, and boundary-radiative heat transfer analysis with the structural analysis of reinforced concrete members. The effect of the models selected for the various temperature-dependent properties of concrete and steel reinforcement on the overall response of reinforced concrete members with various loading and fire scenarios was studied. For concrete materials, the temperature-dependent properties investigated and included the density, thermal conductivity, specific heat capacity, thermal expansion strain, peak compressive stress and the corresponding strain, initial modulus of elasticity, tensile strength, and the shape of the stress-strain curve. For steel reinforcing bars, they included the thermal expansion strain, yield stress, ultimate stress, and Young's modulus. In addition to the heat development phase, the cooling phase was also considered as a fire scenario, where the residual capacity of concrete columns subjected to fire was investigated.*

**Keywords:** ASCE; cooling; Eurocode; fire; heat; structures; thermal.

## INTRODUCTION

Fire causes extensive financial losses due to property damage. It also endangers the life and well-being of occupants. This has driven much interest toward the development of fire-resistant structures. However, with the low probability of fire occurrence, prescriptive design concepts provided by many codes and standards around the world can lead to substantively uneconomic designs. Also, the neglect of the interaction between the different reinforced concrete members in an assembly or an entire building subjected to fire can lead to unsafe designs. Therefore, performance-based design has increasingly become a major means of achieving safe, yet economic, designs for fire-resistant structures. This is why advanced modeling of reinforced concrete structures subjected to fire has been a main focus of researchers and structural engineers for many decades.

Advanced modeling of reinforced concrete structures subjected to fire has been treated by researchers in various ways. The most efficient way is combined thermal and structural analysis, which is a time-stepping procedure where the transient heat transfer analysis is performed at certain time intervals and the results are instantaneously used to perform the structural analysis.

Key elements in combined thermal and structural analysis are the specific models used to define the values of the thermal and mechanical temperature-dependent properties of both concrete and steel reinforcing bars. This paper presents a study of the effect of making different choices among these models on the overall response of reinforced

concrete members. A high degree of sensitivity is illustrated through analyzing various reinforced concrete members that were tested under fire in combined thermal and structural analyses using the models provided by three different codes and comparing the analytical results to the experimental results. The codes compared are the *ASCE Manual of Practice*,<sup>1</sup> the former version of the Eurocode (ENV 1992-1-2:1995<sup>2</sup>), and its current version (EN 1992-1-2:2004<sup>3</sup>).

The combined thermal and structural analyses are carried out using VecTor3,<sup>4,6</sup> a finite element analysis computer program that uses the advanced computational modeling procedure presented by EIMohandes.<sup>4</sup> On the structural analysis level, the modeling procedure uses the Modified Compression Field Theory (MCFT),<sup>7</sup> a well-established concrete model with corroborated performance and intrinsic capabilities in modeling shear mechanisms in reinforced concrete. Also, VecTor3 accounts for numerous advanced behavioral mechanisms experienced by reinforced concrete under various loading conditions. In addition, variations of the thermal, physical, and mechanical temperature-dependent properties experienced by concrete and steel reinforcement when subjected to fire are taken into account.

The combined heat and structural analysis procedure is time stepped, where the results are generated at predefined time steps. The procedure, illustrated in Fig. 1, involves two distinct steps. At first, the finite element model is subjected to a specific temperature-time curve along certain surfaces to simulate the exposure of the member to fire. The procedure follows a transient conductive, boundary-convective, and boundary-radiative heat transfer analysis that is solved through an iterative finite element scheme on the model level and an iterative finite difference analysis scheme for the time discretization. The procedure takes into account the temperature-dependent properties of concrete, including density, thermal conductivity, and specific heat capacity.

The transient heat transfer analysis provides the temperatures at all the nodes comprising the finite element model, which are translated to temperatures of the finite elements. These element temperatures are then used to determine thermal expansion strain and the mechanical properties of the concrete and steel reinforcing bars. The mechanical temperature-dependent properties of concrete include the thermal expansion strain, peak compressive stress and the corresponding strain, initial modulus of elasticity, tensile

*ACI Structural Journal*, V. 113, No. 3, May-June 2016.

MS No. S-2014-176.R1, doi: 10.14359/51688605, received June 27, 2015, and reviewed under Institute publication policies. Copyright © 2016, American Concrete Institute. All rights reserved, including the making of copies unless permission is obtained from the copyright proprietors. Pertinent discussion including author's closure, if any, will be published ten months from this journal's date if the discussion is received within four months of the paper's print publication.

## MODELS COMPARISON SCHEME

Because the combined heat and structural analysis procedure involves two distinct steps, a comparison of the different models of temperature-dependent properties also needs to be carried out in two steps. The first comparison involves the physical and thermal temperature-dependent properties of concrete that affect the transient heat transfer analysis. These properties include the density, thermal conductivity, and specific heat capacity of concrete. The second comparison involves the mechanical temperature-dependent properties of both concrete and steel reinforcing bars. For concrete, these properties include the thermal expansion strain, peak compressive stress and the corresponding strain, initial modulus of elasticity, tensile strength, and the shape of the stress-strain curve. For steel reinforcing bars, they include thermal expansion strain, yield stress, ultimate stress, and Young's modulus.

For a fair comparison of the models defining the mechanical properties of concrete and steel, the same temperature distribution needs to be used for all the structural analyses in which the different mechanical-properties models are used. Thus, after completing the comparison of the models affecting the transient heat transfer analysis, a decision is made regarding which ones yield the most accurate results compared to the experimental results. These models are then used for all the structural analyses carried out afterward. A full list of the models and assumptions of the properties of both concrete and steel reinforcement is provided by ElMohandes.<sup>4</sup>

Three different loading cases and fire scenarios are investigated through three different experimental series conducted by the National Research Council of Canada (NRC):

**Case I:** Reinforced concrete columns under sustained loading during the event of fire, investigated through the experimental series of Columns 10 to 12.<sup>8</sup>

**Case II:** Reinforced concrete columns under sustained axial loading during the event of fire, taking into account the effect of the lateral expansion of slabs, investigated through the testing of Column 1582.<sup>9</sup>

**Case III:** Reinforced concrete columns under sustained axial loading during the event of fire and through the cooling phase, investigated through the experimental series of Columns A and B.<sup>10</sup>

## EXPERIMENTAL SERIES

All three experimental series were conducted on geometrically and structurally identical full-scale column specimens. The columns had a 305 mm (12 in.) square cross section and a height of 3810 mm (12.5 ft). They were reinforced using four 25 mm (1 in.) diameter longitudinal steel bars with a clear cover of 48 mm (1.9 in.), tied using 10 mm (0.4 in.) diameter ties at a spacing of 305 mm (12 in.). Figure 2 shows the reinforcement and cross section of a typical specimen.

For the steel reinforcing bars, only one test was carried out for all the specimens, where the yield stress and the ultimate strength of the longitudinal bars were reported as 444 and 730 MPa (64.4 and 105.9 ksi), respectively, and the yield stress and the ultimate strength of the ties were reported as 427 and 671 MPa (61.9 and 97.3 ksi), respectively.

The simulation of natural fire conditions in the three experimental series was done in the Column Furnace

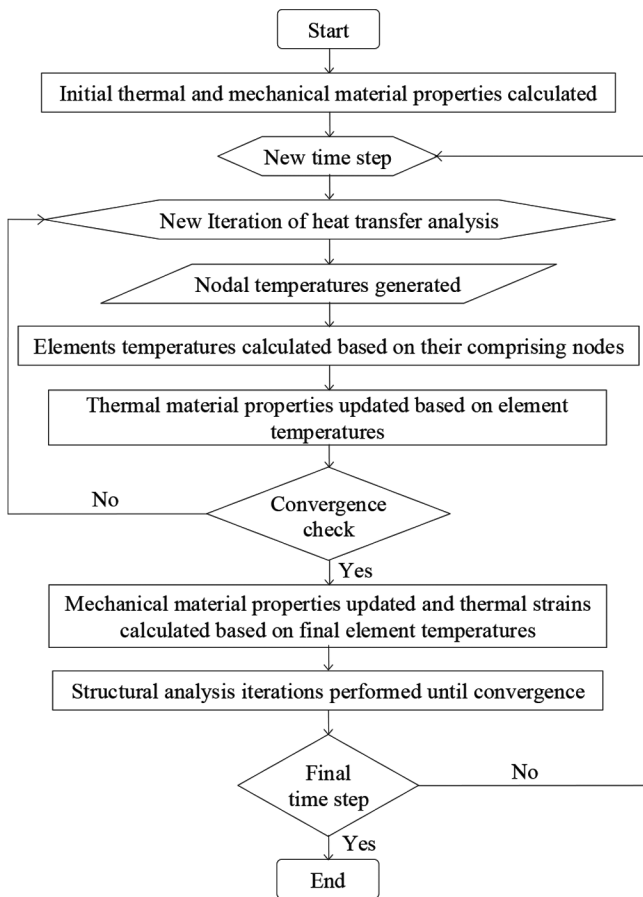


Fig. 1—Flowchart of time-stepping procedure for combined thermal and structural analysis.

strength, and the shape of the stress-strain curve. For steel reinforcing bars, they include thermal expansion strain, yield stress, ultimate stress, and Young's modulus.

The second step in the procedure, repeated during each iteration at each time step, is the structural analysis. The thermal expansion strain and the updated mechanical properties of the finite elements are used in the structural analysis, along with all the other external and internal loading conditions. The analysis is solved through an iterative finite element scheme. The time-stepping structural analysis procedure provides a full structural response of the structure at predefined time intervals, including the failure mode. More details are provided by ElMohandes.<sup>4</sup>

## RESEARCH SIGNIFICANCE

Due to the lack of standardized fire tests for concrete and steel as construction materials, the models available in the literature for defining their various temperature-dependent properties when subjected to fire show evident scatter.

This paper uses a computational modeling procedure recently developed by ElMohandes<sup>4</sup> to show the effect of the variations among these models on the overall response of reinforced concrete members subjected to fire. Models presented by the *ASCE Manual of Practice*,<sup>1</sup> the former version of the Eurocode (ENV 1992-1-2:1995<sup>2</sup>), and its current version (EN 1992-1-2:2004<sup>3</sup>) are used to analyze reinforced concrete members tested under various fire scenarios and different loading conditions.

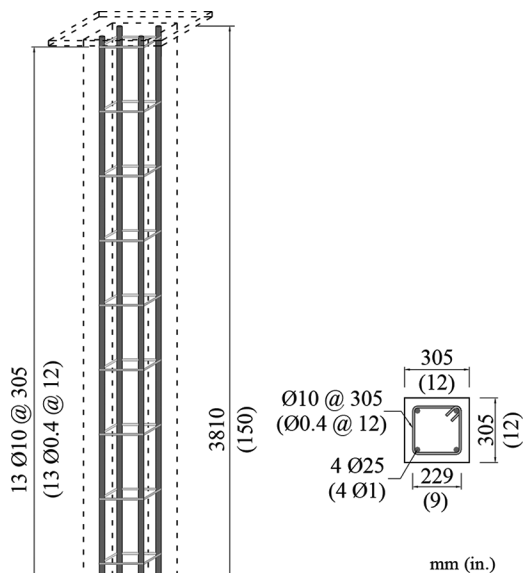


Fig. 2—Reinforcement and cross section of typical NRC column specimen.

Facility of the National Research Council of Canada (NRC). The tests followed the CAN/ULC S101<sup>11</sup> temperature-time model, which is similar to the ASTM E119<sup>12</sup> model, for the ascending temperature branch (fire development phase) and the ISO 834<sup>13</sup> model for the descending temperature branch (fire decay phase).

### NRC COLUMNS 10 TO 12 TESTS

These three columns were constructed and tested by Lie and Lin.<sup>8</sup> On the day of testing, the relative humidity at the centre of Columns 10, 11, and 12, was reported as 75%, 75%, and 76%, respectively, which is equivalent to a moisture content of 3.16%, 3.16%, and 3.20% by weight, respectively. The concrete was mixed with calcareous aggregates and the compressive strengths were 40.9, 36.9, and 40.0 MPa (5.9, 5.4, and 5.8 ksi) for Columns 10, 11, and 12, respectively. Column 10 was loaded to 800 kN (179.8 kip), Column 11 to 1067 kN (239.9 kip), and Column 12 to 1778 kN (399.7 kip), which amounted to 20.4%, 29.7%, and 46.7% of their capacity, respectively, based on a monotonic loading analysis carried out using VecTor3. The test involved loading the columns to the target axial load, then, 1 hour later, subjecting them to the CAN/ULC S101<sup>11</sup> standard temperature-time curve until failure.

To monitor the temperature of concrete through the depth of the columns, four groups of thermocouples were installed at three levels through the height. A group of thermocouples was installed at one-fourth of the height of the columns from the top and another at the same distance from the bottom. Two other groups of thermocouples were installed

at midheight of the column at two diagonally opposite quadrants of the square cross section.

### NRC COLUMN 1582 TEST

This test, carried out by Mostafaei et al.,<sup>9</sup> involved testing a column specimen for fire resistance assessment under both axial and lateral loads. This type of loading profile aims at imitating the loading conditions of columns as parts of buildings, rather than individual members. A column in a building that is exposed to fire would experience differential lateral displacement at its ends due to the thermal expansion of the slabs it connects to at its top and bottom, in turn, inducing significant levels of lateral shear forces.

To estimate the lateral displacement acting on the column specimen, the commercial thermal analysis program SAFIR<sup>14</sup> was used to carry out a finite element analysis for a six-story prototype building for which a compartment fire scenario was assumed. The building had six 9 m (29.5 ft) spans in one direction and four 5 m (16.4 ft) spans in the other. Each of the six stories was 3.8 m (12.5 ft) high, resulting in a total height of 22.9 m (75.0 ft) for the entire building. The compartment selected for the fire scenario was on the first floor in one of the middle spans of one of the shorter edges. The compartment was exposed to the CAN/ULC S101<sup>11</sup> standard temperature-time curve. Column 1582 was selected for the experimental testing as a worst-case scenario, with the maximum axial and lateral load combination.

The concrete was mixed with calcareous aggregates and had a compressive strength of 55.0 MPa (8.0 ksi). The specimen had one group of thermocouples at midheight of the column. On the day of testing, the relative humidity at the center of Column 1582 was reported as 72.8%, which is equivalent to a moisture content of 3.07% by weight. The column was loaded to an axial load of 1590 kN (357.4 kip). This amounted to 31.1% of the column capacity and was applied from the bottom, prior to the start of fire. Rotation was restrained at both ends.

The setup of the test required that the column's top and bottom edges be covered by insulation. Thus, only the middle 3175 mm (10.42 ft) length of the 3810 mm (12.5 ft) long column was subjected to fire. The mechanical and thermal loading setup of Column 1582 is shown in Fig. 3. To allow for a longer fire exposure duration, the lateral displacement applied to the top of the column was approximated and capped at 50 mm (2 in.), following the profile shown in Fig. 4. At 120 minutes from the start of fire and lateral loading application, the maximum lateral displacement of 50 mm (2 in.) was reached. The column was left exposed to fire under the maximum lateral displacement until failure.

### NRC COLUMNS A AND B TESTS

This experimental series, carried out by Lie et al.,<sup>10</sup> was aimed at assessing the residual strength of reinforced concrete columns after exposure to fire. The objective for such an assessment is the determination of the feasibility of repair of fire-damaged structures. Columns A and B were loaded, then subjected to fire, following the CAN/ULC S101<sup>11</sup> standard temperature-time curve, in the testing furnace for 1 and 2 hours, respectively. They were both allowed to cool naturally (in air at room

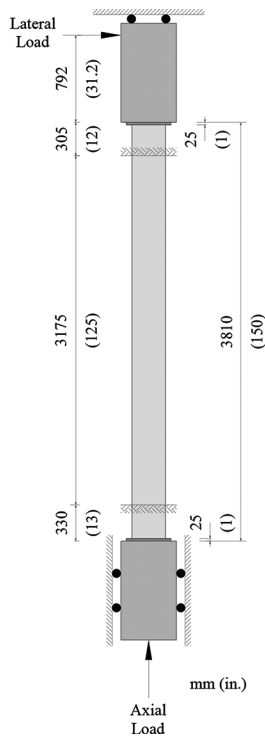


Fig. 3—Mechanical and thermal loading setup of NRC Column 1582.

temperature) for approximately 24 hours until they reached room temperature and then were axially loaded until failure.

The concrete was mixed with siliceous aggregates. On the day of testing, the compressive strength was 38.9 MPa (5.6 ksi) for Column A and 41.8 MPa (6.1 ksi) for Column B. The columns had one group of thermocouples at midheight. The relative humidity at the center of Columns A and B was reported as 87% and 82%, respectively, which is equivalent to a moisture content of 3.66% and 3.45% by weight, respectively. Both columns were loaded axially 1 hour prior to the fire test. Column A was loaded to 992 kN (223 kip) and Column B to 1022 kN (229.8 kip), which amounted to 22.0% and 21.4% of their axial capacity, respectively.

### TRANSIENT HEAT TRANSFER ANALYSIS

Only one-fourth of the cross section of the column specimens was analyzed because the section is symmetric in two directions. The model employed only one element, 25 mm (1 in.) thick, in the longitudinal direction because the heat transfer analysis is transversely bidirectional through the depth of the column. The finite element mesh was chosen such that there was a node at the location of every thermocouple. The distances of the nodes from the surface of the model were 4.4, 6.4, 9.1, 12.8, 17.8, 25.4, 26.7, 38.1, 44.5, 63.5, 71.3, 101.6, 108, and 152.5 mm (0.175, 0.25, 0.36, 0.5, 0.7, 1, 1.05, 1.5, 1.75, 2.5, 2.8, 4, 4.25, and 6 in.). The element discretization distances were identical in both directions.

The *ASCE Manual of Practice*<sup>1</sup> and the former version of the Eurocode (ENV 1992-1-2:1995<sup>2</sup>) provide different models for the thermal properties of concrete mixed with calcareous aggregates and concrete mixed with siliceous aggregates. Therefore, the experiment results of the different experimental series are compared to the analytical results

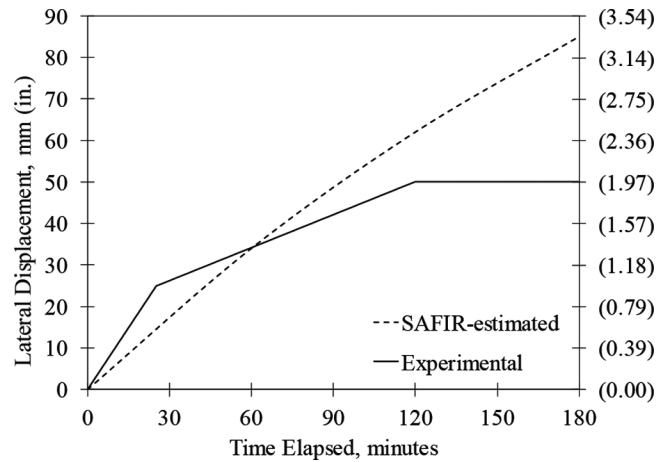


Fig. 4—SAFIR-estimated and experimental lateral loading profile for NRC Column 1582.

generated using the models of the respective type of aggregate. The models provided by the current version of the Eurocode (EN 1992-1-2:2004<sup>3</sup>), however, do not distinguish between concrete mixed with different types of aggregate; hence, the experiment results of all the experimental series are compared to the analytical results generated using these models.

Another major difference between the models is that the former version of the Eurocode (ENV 1992-1-2:1995<sup>2</sup>) and the current version (EN 1992-1-2:2004<sup>3</sup>) recognize the effect of the moisture content of concrete on its specific heat capacity, while the *ASCE Manual of Practice*<sup>1</sup> does not. A moisture content of 4% by weight is chosen for concrete in all the analyses. This moisture content is a reasonable estimate for concrete at a relatively young age and closely matches the values measured on the days of testing.

In all the analyses, for concrete, the convective heat transfer coefficient and the emissivity (for the radiative heat transfer coefficient) were chosen as 25 W/m<sup>2</sup>°C and 0.7, respectively, according to the recommendations of the current version of the Eurocode (EN 1992-1-2:2004<sup>3</sup>). The initial density of concrete was taken as 2400 kg/m<sup>3</sup> (150 lb/ft<sup>3</sup>).

### HEAT TRANSFER IN CALCAREOUS-AGGREGATE SPECIMENS

In the experimental series of Columns 10 to 12<sup>8</sup> and the experimental series of Column 1582,<sup>9</sup> calcareous aggregates were used in the concrete mixture. The results of these two experimental series were used to compare the different models defining the thermal properties of concrete mixed with calcareous aggregates at elevated temperatures.

Figures 5 and 6 show the results of the analysis at depths of 25.4 and 152.5 mm (1 and 6 in.), respectively. For Columns 10 to 12, the results shown represent the average measurements of the thermocouples at the same location for the four groups installed. More results are presented by ElMohandes.<sup>4</sup>

The plots show that the experimental results of Columns 10, 11, and 12 are relatively similar, whereas those of Column 1582 are different. This can be attributed to the fact that Columns 10, 11, and 12 were cast and tested as a part of one test series; hence, the same materials and same test technique were used, while Column 1582 was a part of a different series that was cast and tested many years later.

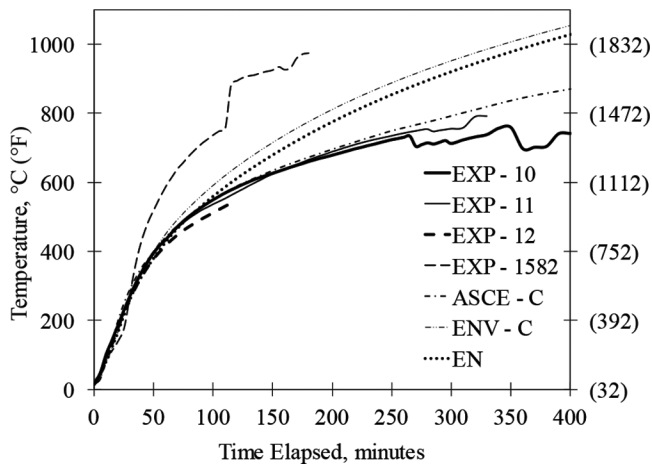


Fig. 5—Temperature change at depth of 25.4 mm (1 in.) for NRC Columns 10, 11, 12, and 1582.

Also, Column 1582 was subjected to lateral loading, which caused significant spalling of the concrete cover over the entire face that was subjected to tension. This would effectively cause the higher temperatures observed in the plots.

Averaging the experimental results of the four different specimens, the mean analytical-to-experimental ratio for the temperatures at a depth of 25.4 mm (1 in.) generated by the models provided by the *ASCE Manual of Practice*,<sup>1</sup> the former version of the Eurocode (ENV 1992-1-2:1995<sup>2</sup>), and its current version (EN 1992-1-2:2004<sup>3</sup>) are 1.04, 1.17, and 1.12, respectively, with coefficients of variation of 6.9%, 11.5%, and 11.8%, respectively. For the temperatures at the centers of the columns, the mean analytical to experimental ratio is 0.92, 1.02, and 0.94, for the three models in the same order, with coefficients of variation of 23.3%, 18.6%, and 18.1%, respectively.

It can be observed that the models provided by the *ASCE Manual of Practice*<sup>1</sup> for concrete mixed with calcareous aggregates manage to accurately estimate the temperature of concrete at a depth of 25.4 mm (1 in.), but not at the centers of the columns where the dispersion is also significantly high. The models provided by the latest version of the Eurocode (EN 1992-1-2:2004<sup>3</sup>) are capable of estimating the experimental temperatures to a lesser extent, but consistently at both depths. However, they manage to capture the kink in the plot at 100°C (212°F) caused by the evaporation of the evaporable water inside the concrete, which is neglected by the models provided by the *ASCE Manual of Practice*.<sup>1</sup>

### HEAT TRANSFER IN SILICEOUS-AGGREGATE SPECIMENS

In the experimental series of Columns A and B,<sup>10</sup> siliceous aggregates were used in the concrete mixture. The results of this experimental series were used to compare the different models defining the thermal properties of concrete mixed with siliceous aggregates at elevated temperatures.

Figures 7 and 8 show the results of the analysis of Column A at depths of 25.4 and 152.5 mm (1 and 6 in.), respectively. Figures 9 and 10 show the results of Column B. More results are presented by ElMohandes.<sup>4</sup> Because the standards under comparison do not present models for the post-fire thermal properties of concrete, it was assumed that the properties follow the same models in the cooling phase until they are

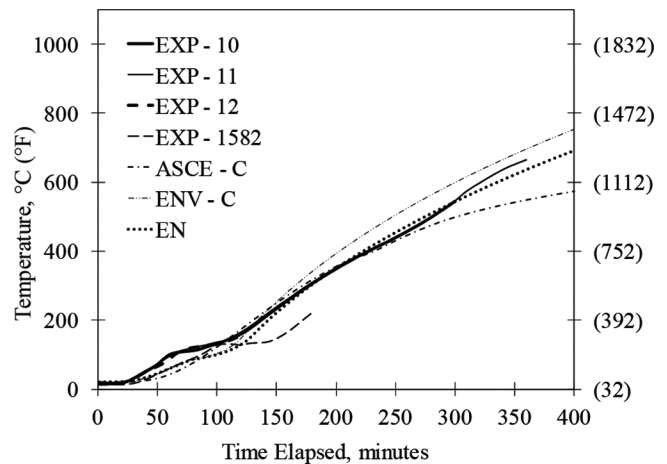


Fig. 6—Temperature change at depth of 152.5 mm (6 in.) for NRC Columns 10, 11, 12, and 1582.

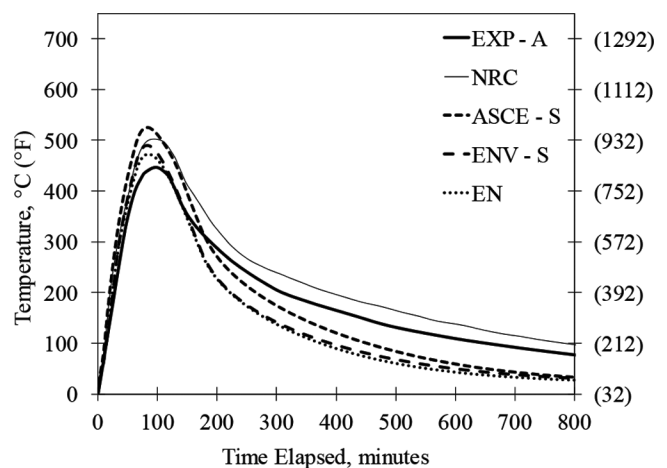


Fig. 7—Temperature change at depth of 25.4 mm (1 in.) for NRC Column A.

fully restored to their pre-fire values when the concrete returns to room temperature.

Figures 7, 8, 9, and 10 also show the analytical estimates presented by Lie et al.,<sup>10</sup> denoted ‘NRC’. These estimates were calculated using the models presented by the *ASCE Manual of Practice*<sup>1</sup> in a finite difference method, based on the procedure presented by Lie and Allen<sup>15</sup> and Lie et al.<sup>16</sup>

The experimental results show that the models presented by the current version of the Eurocode (EN 1992-1-2:2004<sup>3</sup>) are the ones most capable of estimating the experimental results. The average analytical-to-experimental ratios at the two depths presented were 1.10, 1.04, and 1.02 for the three aforementioned standards, respectively. This is based on the comparison of the maximum temperatures measured at the various depths through the columns sections with their respective values estimated by VecTor3.

However, all the models presented tend to significantly underestimate the post-peak temperatures, while the NRC computed values overestimate them but to a lesser extent. Because the NRC estimates were based on analyses using the models presented by the *ASCE Manual of Practice*,<sup>1</sup> yet these estimates differ from the analytical results calculated by VecTor3 using the same models, one may assume that the models are not responsible for this difference. Lie et al.<sup>10</sup>

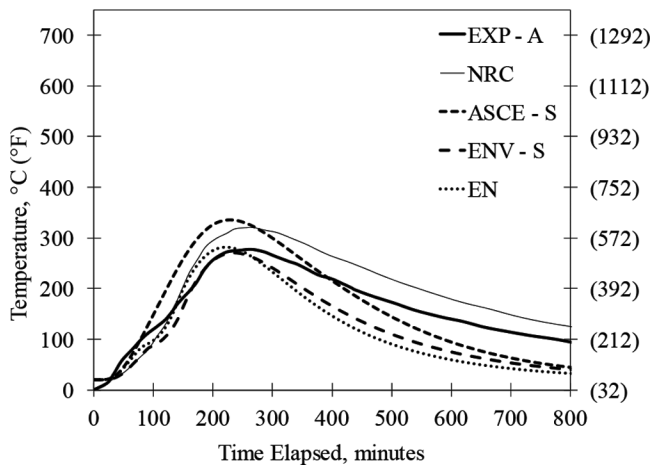


Fig. 8—Temperature change at depth of 152.5 mm (6 in.) for NRC Column A.

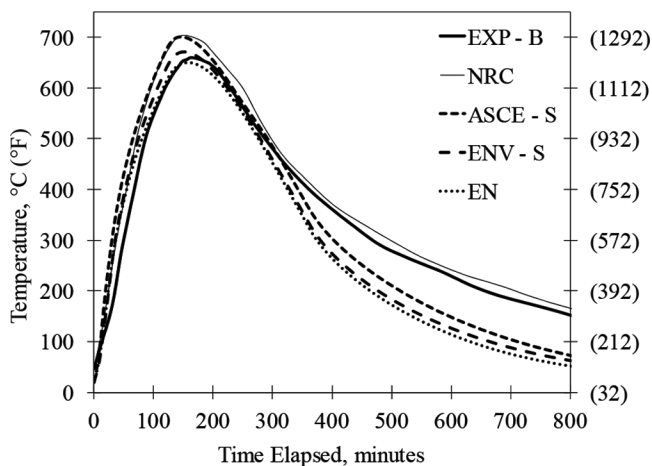


Fig. 9—Temperature change at depth of 25.4 mm (1 in.) for NRC Column B.

stated that measurements were made of the furnace temperatures during the fire exposure and the cooling periods until the average furnace temperature reached near-ambient temperatures, yet they failed to report these temperatures. Therefore, one may surmise that the reason for the difference between the analytical and experimental results can be attributed to a possible difference between the actual furnace temperatures and the ISO 834<sup>13</sup> model that was used in the analysis for the descending temperature branch (fire decay phase).

### COMBINED THERMAL AND STRUCTURAL ANALYSIS

The models provided by the current version of the Eurocode (EN 1992-1-2:2004<sup>3</sup>) proved to produce the most accurate estimation of the temperatures through the depth of concrete, compared to their counterparts in the other two standards. This applies to concrete mixed with both calcareous and siliceous aggregates; hence, it applies to the three experimental series chosen for comparison.

Therefore, the models provided by the Eurocode (EN 1992-1-2:2004<sup>3</sup>) were used for the heat transfer stage of the combined thermal and structural analyses for all the experimental series. This aims at isolating the effect of the different models provided by the three standards for the mechanical

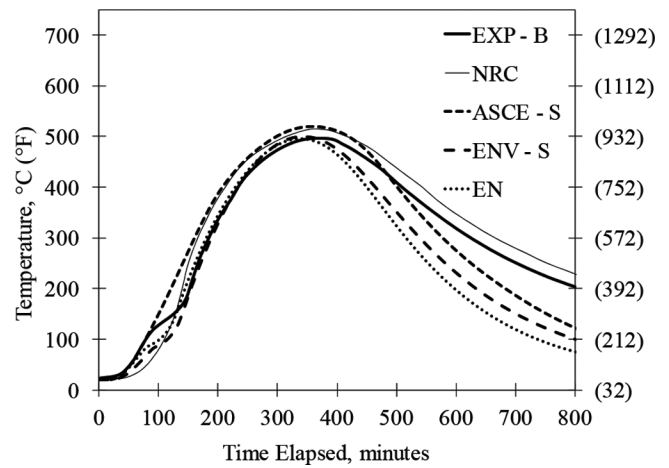


Fig. 10—Temperature change at depth of 152.5 mm (6 in.) for NRC Column B.

properties of concrete and steel reinforcing bars. These models will be used in the structural analysis stage that is undertaken at the end of the heat transfer analysis stage at each time step.

Because the mechanical properties of the steel reinforcing bars are very sensitive to temperature, different finite element discretizations were used. They involved more elements in the concrete cover area to ensure an accurate estimation of the temperatures of the bars.

The deformation of the specimens is governed by a balance between the thermal expansion of steel and concrete, and the deterioration of their stiffnesses. In general, regardless of the level of axial loading the specimens are subjected to, the specimens expand during the first part of the test where the behavior is mainly dominated by the thermal expansion strains while the reduction of the stiffnesses of concrete and steel is not substantial at lower temperatures. In this part, one can notice a kink in the time-displacement plot, which is caused by the yielding of steel reinforcing bars, as the yield stress declines with the increase in temperature.

The expansion reaches a peak after a certain period of time, and then decreases as time passes. After reaching the peak expansion, the stiffnesses of concrete and steel are compromised to the extent that the contraction displacement resulting from the axial loading exceeds the expansion displacement resulting from the increase in temperature. As time passes and the temperatures of the concrete and steel increase, their stiffnesses keep declining until a certain point where their strengths are not sufficient to withstand the axial loads, and the specimen fails.

### NRC COLUMNS 10, 11, AND 12 ANALYSIS

For the finite element discretization chosen for the analyses of these columns, only one-fourth of the column section was modeled, taking advantage of the double symmetry of the geometrical, structural, and loading setup. The mesh used was symmetric, with twelve 5.04 mm (0.2 in.) thick elements, through the depth of the concrete cover to the longitudinal reinforcing bars, and five 18.4 mm (0.72 in.) thick elements for the core region. Figure 11 shows the mesh through a section between the ties, together with the location of the steel reinforcing bar, which is shown as a black circle (not to scale). Longitudinally, 150 elements with a length of 25.4 mm (1 in.)

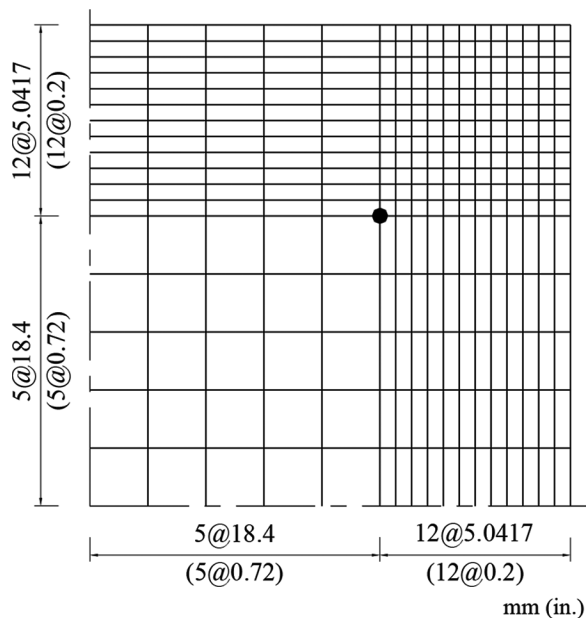


Fig. 11—Finite element discretization for structural analysis for cross section of NRC Columns 10, 11, and 12 at section occurring between ties.

each, were used. The ties were spaced at 305 mm (12 in.); that is, a tie at every 12 layers of elements along the height. The axial load was applied at the top of the column at the center of the cross section. The models were restrained in all directions at their bases. The axial load was kept constant until failure, and a time step of 60 seconds was used for the analysis.

Figures 12, 13, and 14 show the experimental results of the vertical displacement at the top of the columns for Columns 10, 11, and 12, respectively. The figures also show the analytical results estimated by VecTor3 using the models provided by the *ASCE Manual of Practice*,<sup>1</sup> the former version of the Eurocode (ENV 1992-1-2:1995<sup>2</sup>), and its current version (EN 1992-1-2:2004<sup>3</sup>). A positive displacement means expansion along the height of the column, and a negative displacement means contraction. For the analytical results, the displacements shown only represent the change in height from the start of the fire, neglecting the initial displacements resulting from the axial load that was applied an hour prior to the fire exposure.

Table 1 shows the maximum expansion displacement reached,  $d$ , and the time from the start of fire to failure,  $t$ , for Columns 10, 11, and 12. For the maximum expansion displacement, all the models manage to estimate its value with reasonable accuracy. A general trend of underestimation is evident in the case of the Eurocode (ENV 1992-1-2:1995<sup>2</sup>), with a mean analytical-to-experimental ratio of 0.85 and a coefficient of variation of 20%. With the *ASCE Manual of Practice*,<sup>1</sup> there is a general trend of overestimation, with a mean analytical-to-experimental ratio of 1.26 and a coefficient of variation of 14%. The models provided by the Eurocode (EN 1992-1-2:2004<sup>3</sup>), on the other hand, managed to capture the maximum expansion displacement more precisely, with a mean analytical-to-experimental ratio of 0.97 and a coefficient of variation of 2%.

However, the models provided by the Eurocode (EN 1992-1-2:2004<sup>3</sup>) do not estimate the time from the

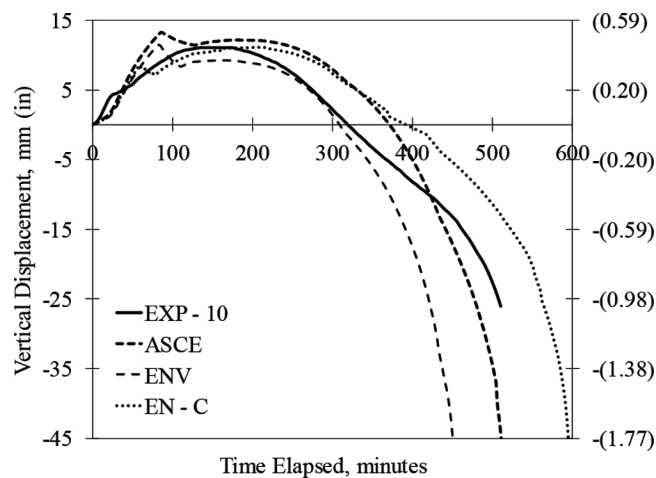


Fig. 12—Vertical displacement of NRC Column 10 from start of fire to failure.

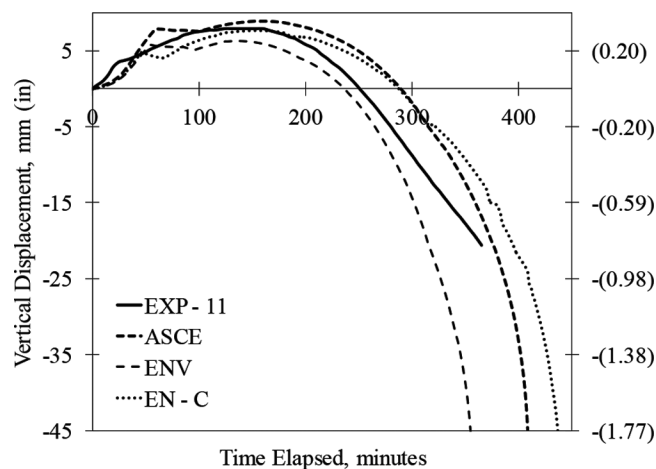


Fig. 13—Vertical displacement of NRC Column 11 from start of fire to failure.

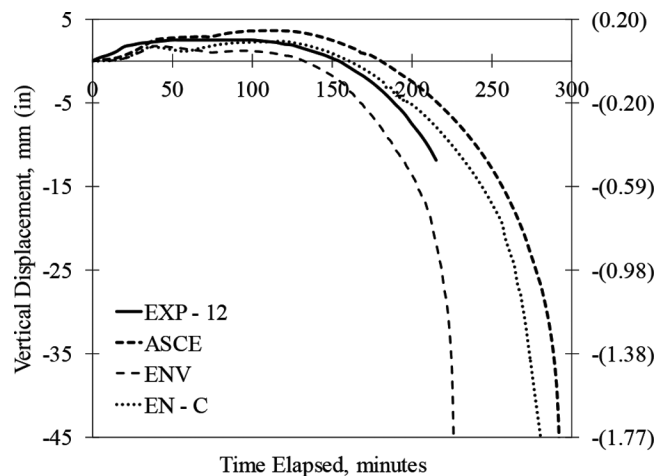


Fig. 14—Vertical displacement of NRC Column 12 from start of fire to failure.

start of fire to failure within a reasonable range of accuracy, giving an unsafe overestimation with a mean analytical-to-experimental ratio of 1.25 and a coefficient of variation of 8%. The models provided by the *ASCE Manual of Practice*<sup>1</sup> also overestimate the time to failure with a mean

**Table 1—Experimental and analytical results of Columns 10, 11, and 12**

Specimen	Experimental results		<i>ASCE Manual of Practice</i> <sup>1</sup>		ENV 1992-1-2:1995 <sup>2</sup>		EN 1992-1-2:2004 <sup>3</sup>	
	<i>d</i> , mm (in.)	<i>t</i> , min	<i>d</i> , mm (in.)	<i>t</i> , min	<i>d</i> , mm (in.)	<i>t</i> , min	<i>d</i> , mm (in.)	<i>t</i> , min
Col. 10	11.10 (0.44)	510	12.15 (0.48)	517	9.21 (0.36)	455	11.06 (0.04)	598
Col. 11	7.90 (0.31)	365	8.94 (0.35)	411	6.32 (0.25)	359	7.71 (0.3)	443
Col. 12	2.50 (0.1)	215	3.65 (0.14)	295	1.77 (0.07)	228	2.37 (0.09)	294

analytical-to-experimental ratio of 1.17 and a coefficient of variation of 16%. The models that manage to capture the time of failure more precisely are the ones provided by the Eurocode (ENV 1992-1-2:1995<sup>2</sup>), estimating it with a mean analytical-to-experimental ratio of 0.98 and a coefficient of variation of 9%.

### NRC COLUMN 1582 ANALYSIS

The quarter cross section finite element model created for the analysis of Columns 10, 11, and 12 could not be used for the analysis of Column 1582. The bending moment ensuing from the lateral loading required the entire depth of the column to be modeled. Therefore, half of the cross section was modeled, using the same finite element discretization described previously for Columns 10, 11, and 12. Longitudinally, the column was discretized into 75 elements with a height of 50.13 mm (1.97 in.) each, to achieve a total height of 3810 mm (150 ft) for the model. The 13 ties were modeled at 300 mm (11.8 in.), instead of the actual 305 mm (12 in.), to fit in the selected finite element discretization. This means that a tie was located at every sixth element along the height.

A time step of 60 seconds was used for the analysis. The axial load of 1590 kN (357.4 kip) was applied prior to the start of the fire at the top of the column. The exact lateral loading profile applied during the test was applied at the top of the column in a displacement control loading scheme until failure. The thermal loading of the fire and the lateral loading were started at the same time, resembling the experimental conditions.

Figure 15 shows the experimental results for the vertical displacement at the top of Column 1582 compared to the analytical results estimated using the models presented by the *ASCE Manual of Practice*,<sup>1</sup> the former version of the Eurocode (ENV 1992-1-2:1995<sup>2</sup>), and its current version (EN 1992-1-2:2004<sup>3</sup>), respectively.

It should be noted that the test results showed an initial lateral load of approximately 14 kN (7.2 kip) after applying the axial load but before the start of the fire or the application of the lateral displacement. This initial lateral load might be a result of a slightly eccentric axial loading or some imperfections in the specimen construction or in the loading mechanism. To be able to compare the experimental results to the analytical results calculated by VecTor3, this initial lateral load has been deducted from all the lateral loads reported throughout the test.

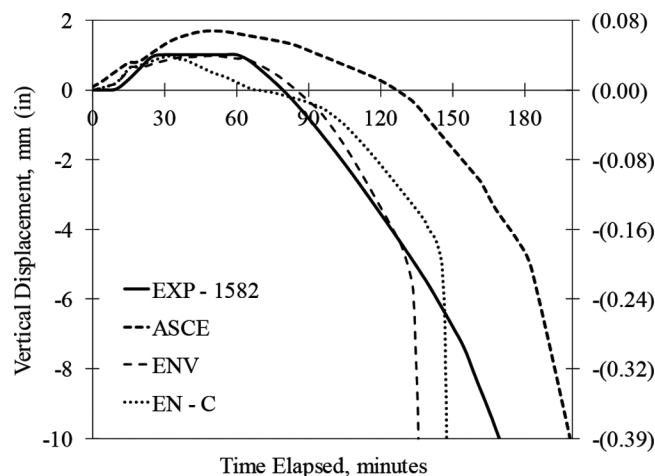


Fig. 15—Vertical displacement of NRC Column 1582 from start of fire to failure.

The models provided by the former version of the Eurocode (ENV 1992-1-2:1995<sup>2</sup>) and the ones provided by its current version (EN 1992-1-2:2004<sup>3</sup>) tend to estimate the time of failure from the start of fire on the conservative side, with an analytical-to-experimental ratio of 0.76 and 0.82, respectively. On the other hand, the models provided by the *ASCE Manual of Practice*<sup>1</sup> tend to estimate a fire resistance that is longer in time than the experimental fire resistance with an analytical-to-experimental ratio of 1.13.

The models provided by the former version of the Eurocode (ENV 1992-1-2:1995<sup>2</sup>) seem to generate the most accurate deformations, with an analytical-to-experimental ratio of 0.96 for the maximum expansion displacement, followed by those provided by the current version (EN 1992-1-2:2004<sup>3</sup>) with an analytical-to-experimental ratio of 0.95 for the same displacement. The models provided by the *ASCE Manual of Practice*<sup>1</sup> tend to estimate significantly higher expansion displacements, with an analytical-to-experimental ratio of 1.68.

### NRC COLUMNS A AND B ANALYSIS

The finite element model created for the analyses of Columns 10, 11, and 12 was used in the analysis of Columns A and B. A time step of 60 seconds was used. The models of Columns A and B were loaded to their respective axial load, then subjected to the CAN/ULC S101<sup>11</sup> standard temperature-time curve for 1 and 2 hours, respectively. Then, the fire was allowed to decay following the ISO 834<sup>13</sup> standard temperature-time curve for the descending temperature branch (fire decay phase). For the post-fire residual mechanical properties of concrete, the models presented by Chang et al.<sup>17</sup> were used. For steel reinforcing bars, it was assumed that the mechanical properties were fully recovered to their initial pre-fire values when they cooled to room temperature.

It should be noted that the literature presents models for the mechanical properties of concrete and steel at elevated temperatures during the event of fire and other models for the residual mechanical properties after the event of fire. Yet, there is a void in the literature for the cooling period and the path that the mechanical properties follow, going from their values at the maximum reached temperature to their values when they cool to room temperature (residual properties).

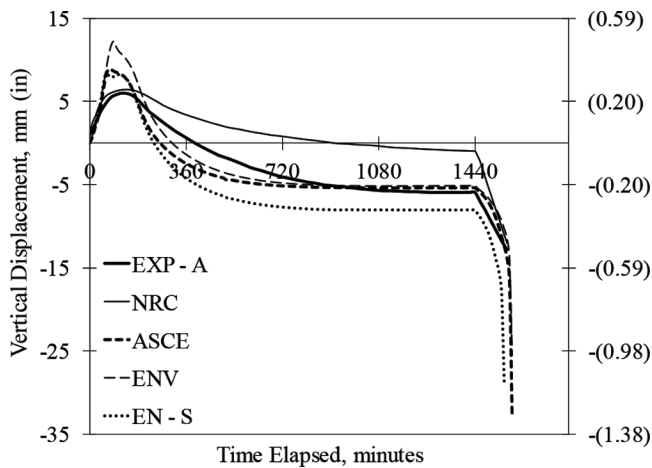


Fig. 16—Vertical displacement of NRC Column A from start of fire to failure.

Therefore, in this study, for the lack of a better experimentally proven method, it has been assumed that the mechanical properties of concrete and steel change linearly moving between the values mentioned previously.

Figures 16 and 17 show the vertical displacements of Columns A and B from the start of the fire, respectively. The analytical results estimated using the three sets of models to be compared are presented, together with the experimental results and the analytical estimate provided by Lie et al.,<sup>10</sup> denoted ‘NRC’. This analytical estimate was derived by using the experimentally measured temperatures of concrete at different depths from the surface to divide the section into zones based on the maximum temperature reached. Then, the mechanical properties of these zones were determined using the available models for residual properties. Finally, a finite element analysis was undertaken for a model constructed with these residual mechanical properties and the failure load was determined.

While examining Fig. 16 and 17, one should recall that the temperatures of concrete through the section that were analytically calculated were consistently below the experimental ones. This might explain why the analytically estimated displacements of Columns A and B decreased at a steeper rate than the experimental displacements. Other reasons may be the limited data used to develop the models describing the post-fire properties and the approximate procedure adopted to fill the cooling phase properties void that was explained previously.

Figure 16 shows that, for Column A, the *ASCE Manual of Practice*<sup>1</sup> and the former version of the Eurocode (EN 1992-1-2:1995<sup>2</sup>) accurately estimate the residual displacement after cooling, while the current version of the Eurocode (EN 1992-1-2:2004<sup>3</sup>) overestimates it. However, for Column B, all models seem to significantly underestimate the residual displacement, as can be seen in Fig. 17. For both columns, the maximum expansion displacements are overestimated, with the Eurocode (EN 1992-1-2:1995<sup>2</sup>) estimating significantly higher displacements.

The NRC estimate seems to capture the peak expansion displacements accurately, yet the residual displacements estimates are highly inaccurate. It is unclear why the NRC estimate for Column B estimated that the specimen expanded again while it was cooling.

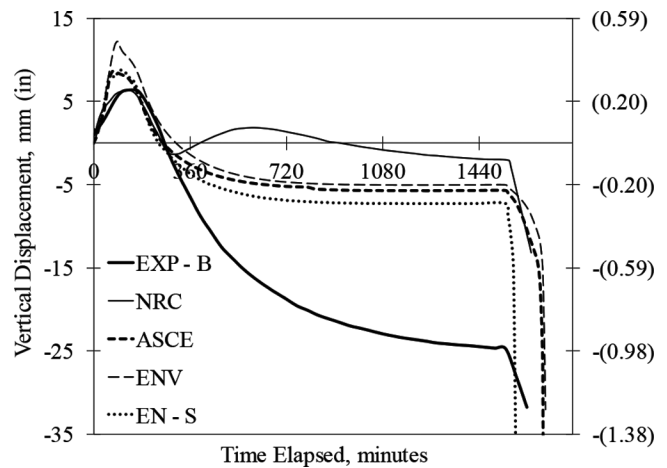


Fig. 17—Vertical displacement of NRC Column B from start of fire to failure.

**Table 2—Experimental and analytical results of Columns A and B**

Specimen	Experimental results, kN (kip)	<i>ASCE Manual of Practice</i> <sup>1</sup> , kN (kip)	ENV 1992-1-2:1995 <sup>2</sup> , kN (kip)	EN 1992-1-2:2004 <sup>3</sup> , kN (kip)
Col. A	1987 (446.7)	2684 (603.4)	2686 (603.8)	2330 (523.8)
Col. B	2671 (600.5)	2700 (607)	2830 (636.2)	2908 (653.7)

Table 2 shows the experimentally determined residual capacity of the columns and the analytically estimated values, based on the different models. The analyses that were carried out using the models presented by the *ASCE Manual of Practice*<sup>1</sup> produced a mean analytical-to-experimental value of 1.18. With the models presented by the former version of the Eurocode (EN 1992-1-2:1995<sup>2</sup>), this value was 1.21. Finally, with the models presented by the current version of the Eurocode (EN 1992-1-2:2004<sup>3</sup>), this value came to 1.13. Hence, one can conclude that the models presented by the current version of the Eurocode (EN 1992-1-2:2004<sup>3</sup>) provide the most accurate results for concrete mixed using siliceous aggregates.

## SUMMARY AND CONCLUSIONS

The finite element structural analysis computer program VecTor3<sup>4-6</sup> was used to study the consequences of making different choices among the models available for the various temperature-dependent properties of concrete and steel reinforcement subjected to fire. Three sets of models from three different codes defining these properties were compared, namely, the *ASCE Manual of Practice*,<sup>1</sup> the former version of the Eurocode (EN 1992-1-2:1995<sup>2</sup>), and its current version (EN 1992-1-2:2004<sup>3</sup>).

Thermal temperature-dependent properties of concrete including density, thermal conductivity, and specific heat capacity, were studied through transient heat transfer analyses. Mechanical temperature-dependent properties of concrete and steel reinforcing bars were studied through combined thermal and structural analyses. They included thermal expansion strain, peak compressive stress and the corresponding strain, initial modulus of elasticity, tensile strength, and the shape of the stress-strain curve for concrete; and thermal expansion

strain, yield stress, ultimate stress, and Young's modulus for steel reinforcing bars. Different loading cases and fire scenarios were analyzed and compared to experimental results.

The results showed that, as a general rule for transient heat transfer analysis, the models provided by the current version of the Eurocode (EN 1992-1-2:2004<sup>3</sup>) yielded the most accurate results compared to the experimental results. This is a general recommendation for concrete members regardless of the type of aggregate used in the concrete mixture. However, the models provided by the ASCE Manual of Practice<sup>1</sup> managed to estimate the results more accurately than those provided by the current version of the Eurocode (EN 1992-1-2:2004<sup>3</sup>) for concrete mixed with calcareous aggregates. However, the models it provided for concrete mixed with siliceous aggregates were not as successful.

For the models defining the mechanical temperature-dependent properties of concrete and steel reinforcing bars, the former version of the Eurocode (ENV 1992-1-2:1995<sup>2</sup>) yielded the most accurate estimates for the time of failure from the start of fire for concrete mixed with calcareous aggregates. However, for the same type of concrete, the models provided by the current version of the Eurocode (EN 1992-1-2:2004<sup>3</sup>) yielded better estimates for the maximum deformation reached throughout the fire. The models provided by the ASCE Manual of Practice<sup>1</sup> yielded the least accurate estimates in terms of both the time of failure and the maximum deformation reached.

For concrete mixed with siliceous aggregates, the models provided by both the ASCE Manual of Practice<sup>1</sup> and the current version of the Eurocode (EN 1992-1-2:2004<sup>3</sup>) provided reasonable estimates of the maximum deformation reached as opposed to those provided by the former version of the Eurocode (ENV 1992-1-2:1995<sup>2</sup>). Also, using the same set of models for residual properties of concrete and steel reinforcement bars, the models provided by the current version of the Eurocode (EN 1992-1-2:2004<sup>3</sup>) managed to give the best estimates of the residual post-fire strength of the reinforced concrete columns tested.

As a general conclusion, although the models provided by the current version of the Eurocode (EN 1992-1-2:2004<sup>3</sup>) have some deficiencies, they are the closest to being capable of generating accurate estimates of the response of reinforced concrete structure subjected to fire. However, the models still do not provide the level of confidence required for a reliable performance-based design. Additional experimental and analytical research is required to develop more reliable models for both the thermal and the mechanical temperature-dependent properties of concrete and steel reinforcing bars.

## NOTATION FOR FIGURES

EXP - 10: experimental results of NRC Column 10; EXP - 11: experimental results of NRC Column 11; EXP - 12: experimental results of NRC Column 12; EXP - 1582: experimental results of NRC Column 1582; EXP - A: experimental results of NRC Column A; EXP - B: experimental results of NRC Column B; ASCE: analytical results estimated by VecTor3 using the models provided by the ASCE Manual of Practice<sup>1</sup>; ENV: analytical results estimated by VecTor3 using the models provided by the former version of the Eurocode (ENV 1992-1-2:1995<sup>2</sup>); EN: analytical results estimated by VecTor3 using the models provided by the current version of the Eurocode (EN 1992-1-2:2004<sup>3</sup>); C: analytical results estimated by VecTor3 using the models of concrete mixed with calcareous aggregates; S: analytical results estimated by VecTor3 using the models of concrete mixed with siliceous

aggregates; NRC: analytical results estimated by the National Research Council of Canada (NRC).

## AUTHOR BIOS

*ACI member Fady ElMohandes is a Structural Engineer at AECOM, Markham, ON, Canada. He received his PhD from the University of Toronto, Toronto, ON, Canada, in 2013. His research interests include computational modeling and performance assessment and analysis of reinforced concrete structures and their behavior under fire and extreme loads.*

*Frank J. Vecchio, F.ACI, is a Professor of civil engineering at the University of Toronto. He is a member of Joint ACI-ASCE Committees 441, Reinforced Concrete Columns, and 447, Finite Element Analysis of Reinforced Concrete Structures. He received the 1998 ACI Structural Research Award, the 1999 ACI Structural Engineer Award, and the 2011 ACI Wason Medal for Most Meritorious Paper. His research interests include advanced constitutive modeling and analysis of reinforced concrete, assessment and rehabilitation of structures, and response under extreme loads.*

## REFERENCES

- Lie, T. T., "Structural Fire Protection," *ASCE Manuals and Reports on Engineering Practice No. 78*, American Society of Civil Engineers, Reston, VA, 1992, 241 pp.
- CEN, "ENV 1992-1-2:1995—Eurocode 2: Design of Concrete Structures—Part 1-2: General Rules. Structural Fire Design," European Committee for Standardization (CEN), Brussels, Belgium, 1996, 63 pp.
- CEN, "EN 1992-1-2:2004—Eurocode 2: Design of Concrete Structures—Part 1-2: General Rules. Structural Fire Design," European Committee for Standardization (CEN), Brussels, Belgium, 2005, 97 pp.
- ElMohandes, F., "Advanced Three-Dimensional Nonlinear Analysis of Reinforced Concrete Structures Subjected to Fire and Extreme Loads," PhD thesis, University of Toronto, Toronto, ON, Canada, 2013, 407 pp.
- ElMohandes, F., and Vecchio, F. J., "Vector3: A. User's Manual," Department of Civil Engineering, University of Toronto, Toronto, ON, Canada, 2013, 81 pp.
- ElMohandes, F., and Vecchio, F. J., "Vector3: B. Sample Coupled Thermal and Structural Analysis," Department of Civil Engineering, University of Toronto, Toronto, ON, Canada, 2013, 68 pp.
- Vecchio, F. J., and Collins, M. P., "The Modified Compression Field Theory for Reinforced Concrete Elements Subjected to Shear," *ACI Journal Proceedings*, V. 83, No. 2, Mar.-Apr. 1986, pp. 219-231.
- Lie, T. T., and Lin, T. D., "Fire Tests on Reinforced Concrete Columns, Specimens No. 1-12," 12 NRC Publications—DBR Internal Reports No. 478-489, Division of Building Research, National Research Council of Canada (NRC), Ottawa, ON, Canada, 1983.
- Mostafaie, H.; Leroux, P.; and Lafrance, P.-S., "Fire Endurance of a Reinforced Concrete Column under Both Axial and Lateral Loads," *NRC Report IRC-RR-327*, National Research Council Canada (NRC), Ottawa, ON, Canada, 2012, 31 pp.
- Lie, T. T.; Rowe, T. J.; and Lin, T. D., "Residual Strength of Fire-Exposed Reinforced Concrete Columns," *Evaluation and Repair of Fire Damage to Concrete*, SP-92, American Concrete Institute, Farmington Hills, MI, 1986, pp. 153-174.
- CAN/ULC S101-07, "Standard Methods of Fire Endurance Tests of Building Construction and Materials," Underwriters Laboratories of Canada, Toronto, ON, Canada, 2007, 85 pp.
- ASTM E119-12a, "Standard Test Methods for Fire Tests of Building Construction and Materials," ASTM International, West Conshohocken, PA, 2012, 34 pp.
- ISO, "ISO 834-1:1999: Fire-Resistance Tests—Elements of Building Construction—Part 1: General Requirements," ISO, Geneva, Switzerland, 1999, 25 pp.
- Franssen, J.-M., "SAFIR: A Thermal/Structural Program Modelling Structures under Fire," North American Steel Construction Conference (NASCC), American Institute of Steel Construction, Chicago, IL, 2003.
- Lie, T. T., and Allen, D. E., "Calculations of the Fire Resistance of Reinforced Concrete Columns," NRCC 12797, Division of Building Research, National Research Council of Canada, Ottawa, ON, Canada, 1972.
- Lie, T. T.; Lin, T. D.; Allen, D. E.; and Abrams, M. S., "Fire Resistance of Reinforced Concrete Columns," *DBR Paper No. 1167*, Division of Building Research, National Research Council of Canada (NRC), Ottawa, ON, Canada, 1984, 20 pp.
- Chang, Y. F.; Chen, Y. H.; Sheu, M. S.; and Yao, G. C., "Residual Stress-Strain Relationship for Concrete after Exposure to High Temperatures," *Cement and Concrete Research*, V. 36, No. 10, 2006, pp. 1999-2005. doi: 10.1016/j.cemconres.2006.05.029

Reproduced with permission of the copyright owner. Further reproduction prohibited without permission.